Talanta 222 (2021) 121487

Contents lists available at ScienceDirect

Talanta

journal homepage: www.elsevier.com/locate/talanta

Fabrication of electrochemical immunosensor based on acid-substituted poly(pyrrole) polymer modified disposable ITO electrode for sensitive detection of CCR4 cancer biomarker in human serum

Elif Burcu Aydın [a,*], Muhammet Aydın [a], Mustafa Kemal Sezgintürk [b]

[a] Tekirdağ Namık Kemal University, Scientific and Technological Research Center, Tekirdağ, Turkey
[b] Çanakkale Onsekiz Mart University, Faculty of Engineering, Bioengineering Department, Çanakkale, Turkey

ARTICLE INFO

Keywords:
CC chemokine Receptor 4
Acid-substituted-polypyrrole P(Pyr-Pac) polymer
Conjugated polymers

ABSTRACT

This study described the first impedimetric immunosensor reported for the determination of CCR4, a new prostate cancer biomarker. This impedimetric immunosensor was constructed through the modification of disposable indium tin oxide (ITO) sheet with a conjugated pyrrole polymer P(Pyr-Pac) and subsequent immobilization of anti-CC chemokine receptor 4 (CCR4) antibodies. Acid-substituted poly(pyrrole) P(Pyr-Pac) polymer contained a lot of carboxyl groups on its end site, which were suitable for attachment of anti-CCR4 antibodies. Electrochemical impedance spectroscopy (EIS) and cyclic voltammetry (CV) were chosen to investigate electrode preparation stages and, EIS was chosen to detect the CCR4 concentration. Anti-CCR4 antibody attached biosensing surface was highly selective to CCR4 antigen, the specific interaction resulted changes in electrochemical signal. Optimization studies containing polymer amount, anti-CCR4 antibody concentration, anti-CCR4 antibody immobilization time and anti-CCR4 antibody-CCR4 antigen interaction time were studied. The developed immunosensor displayed a linear increase with concentrations of CCR4 antigen (0.02–8 pg/mL) and a low detection limit of 6.4 fg/mL. In addition, this biosensor had great reproducibility and repeatability. Moreover, the designed biosensor was successfully used for the quantification of CCR4 antigen in serum samples. The recovery for the spiked serum samples was between 98.25% and 103.99%. The suggested immunosensor illustrated a good selectivity towards some interferents including different biomarkers. This study could establish a new approach for future cancer biomarker detection.

1. Introduction

Prostate cancer (PCa) is a common type of cancer in men. According to estimates from the World Health Organization (WHO) in 2018, 1.3 million new PCa cases have been found in the world. In addition, prostate cancer causes the death to approximately 10% of all cancer patients. The most effective method to decrease PCa mortality rate is early diagnosis of this disease [1]. In order to detect PCa cases, imaging techniques are considered as the most precise techniques. Other PCa diagnostic techniques are ultrasonography, computed tomography, magnetic resonance imaging and cancer immunosorbent assay [2]. Although these methods are robust and highly effective for PCa detection, but most of these techniques have some drawbacks such as low sensitivity, limited specificity and long assay procedure [3,4]. In addition, the sensitivities of these methods are not acceptable [5,6]. Biomarkers are biological molecules which give information about any biochemical processes formed in the human body. In the case of PCa diagnosis, biomarkers have a significant role in screening, diagnosis and prognosis of cancer. PCa biomarkers are originated from the process of ribose nucleic acid, modifications of DNA and metabolites of DNA [3,4]. PCa biomarkers are usually analyzed in human serum and urine. Experimental studies illustrated that PSA is a potential biomarker for PCa and PSA level in serum is a sign of diagnosis and monitoring of PCa [7]. However, PSA is not cancer-specific and various non-malignant circumstances such as benign prostatic hyperplasia and prostatitis can cause a rise in PSA levels [4,8]. In addition, PSA has low specificity for PCa upon prostate biopsies, and therefore, other methods digital rectal examination and transrectal ultrasound are used in addition to the PCa detection [9,10].

Chemokines are a group of small cytokines [11] and they have role in

* Corresponding author.
E-mail addresses: b_e_bahadir@hotmail.com, ebbahadir@nku.edu.tr (E.B. Aydın).

https://doi.org/10.1016/j.talanta.2020.121487
Received 11 April 2020; Received in revised form 20 July 2020; Accepted 29 July 2020
Available online 7 August 2020

migration of different leukocyte populations [12]. Chemokines include four subfamilies: CC, CXC, C and CXC3 [13]. In addition, chemokines have an important role in homeostasis, immunity, cell growth, differentiation and activation [14]. Chemokines and their receptors implicate in the pathogenesis of many inflammatory and infectious diseases including rheumatoid arthritis, asthma, malaria, AIDS and cancer [15,16]. The expression of chemokines and their receptors is regulated in malignant cells via inactivation of tumor suppressor genes, activation of oncogenes and expression of transcription factors [17]. CC chemokine receptor 4 (CCR4) is a basic chemokine receptor and regulates immune homeostasis. CCR4 is expressed on Th2 cells and regulatory T cells. In addition, CCR4 is a biomarker of gastric cancer, breast cancer, head and rack squamous cell carcinoma and prostate cancer [12,18,19]. Various immunoassay methods have been usually used for detection of CCR4, and enzyme-linked immunosorbent assay (ELISA) is the most famous immunoassay technique. ELISA kits are in sandwich-type configurations and include anti-CCR4 capture antibodies, biotinylated anti-CCR4 antibody and peroxidase-streptavidin conjugates. These kits have wide detection range and low detection limit at pg/mL level. The basic disadvantage of this method is the long analysis time (4.5 h). In addition, this method is complex, laborious and high-cost. Therefore, simple, low-cost and ultrasensitive methods are required for CCR4 detection. Electrochemical detection techniques have attracted interest due to their benefits such as excellent sensitivity, low detection limit, rapid analysis procedure and low cost. Electrochemical methods have been used for the detection of various molecules in industry and clinic so far. Electrochemical immunosensors measure the interaction between antibody and antigen and they are usually utilized for different biomarkers detection [20–22]. However, a biosensor for the determination of CCR4 has not been previously developed in literature.

Different materials including polymers, sol-gels and conducting polymers have been employed to increase the stability of the biorecognition molecules utilized in the construction of the biosensors. In this sense, polymers are the best candidate matrices for the biosensor construction [23]. Additionally, biorecognition molecule attachment is the key-stage in biosensor fabrication and a lot of different immobilization matrices have been utilized so far [21,22,24]. Conjugated polymers are organic molecules which have an extended Π-orbital system. Conjugated polymers have flexibility in chemical structures and this property provides easy modification, thus, the required electronic and mechanical properties is formed [25]. Sensors and biosensors are the most popular application area of conjugated polymers [26,27]. The unique features such as rapid electron transfer, high sensitivity, high specificity and good biocompatibility of conjugated polymers make them suitable matrices for biomolecules immobilization [23,28]. Moreover, conjugated polymers can be modified for immobilization of biomolecules. Polypyrrole is one of the most attractive conjugated polymer, and it is utilized mostly in biosensors and immunosensors due to the good biocompatibility and the simple immobilization of several biomolecules [29]. Polypyrrole has been successfully applied for selective detection of glucose [30–32], phosphate [33], tyramine [34,35], anti-cancer drug [36], neurotransmitter [37] and catechol [38]. In these studies, PPy acts as a good transducer matrix for biorecognition element immobilization. Acid-substituted poly(pyrrole) P(Pyr-Pac) polymer contains a lot of carboxyl groups, which are suitable for attachment of biomolecules. P(Pyr-Pac) is a conjugated polymer and it provides more conductive matrix than other matrix materials. In addition, the preparation cost of polymer modified electrode is low and therefore, it provides low-cost analysis.

In this work, P(Pyr-Pac) polymer was successfully self-assembled onto the surface of ITO electrode and employed as an immobilization material for anti-CCR4 antibodies. ITO electrode was a low-cost substrate and therefore, it was chosen as an immobilization platform instead of gold or platinum electrode. By using polymer P(Pyr-Pac) as an immobilization matrix, the surface area of the immunosensor and the active sides for biorecognition element increased. Therefore, the conjugated P(Pyr-Pac) polymer containing carboxyl side groups was synthesized to increase the amount of the attachment points for anti-CCR4 antibody. The electrochemical biosensing ability towards CCR4 antigen were tested via signal measurement of anti-CCR4 antibodies attached electrode. Anti-CCR4 antibody immobilized ITO electrode illustrated high selectivity to CCR4 antigen, resulting to change the electrochemical signal remarkably. Under the optimum experimental conditions, the EIS response increases with increasing of CCR4 concentration. The suggested CCR4 biosensing tool was employed to determine CCR4 antigen in human serum, which confirmed the promising practical application of electrochemical biosensors.

2. Experimental

2.1. Reagents

1-(2-Cyanoethyl)pyrrole, potassium bromide, potassium hydroxide, 4-dimethylamino pyridine, anhydrous iron(III) chloride, *N*-Hydroxysuccinimide (NHS), 1-ethyl-3-(dimethyl-aminopropyl) carbodiimide hydrochloride (EDC), nitromethane, tetrahydrofuran, hydrochloric acid (HCl), dimethylsulfoxide (DMSO), acetone, sulfuric acid (H_2SO_4), potassium chloride, sodium dihydrogen phosphate, di-sodium hydrogen phosphate, potassium ferrocyanide ($K_4[Fe(CN)_6]$) and potassium ferricyanide ($K_3[Fe(CN)_6]$) were purchased from Sigma-Aldrich (USA). Indium tin oxide coated polyethylene terephthalate film substrates (5 mm × 20 mm), monoclonal anti-CC chemokine receptor 4 antibody, CC chemokine receptor 4 antigen and bovine serum albumin (BSA) were from Sigma-Aldrich (USA). All protein solutions were prepared by using 50 mM PBS buffer (pH 7.4). Melanoma-associated antigen 1 (MAGE 1), p22-activated kinase 2 (PAK 2) and cadherin-like protein 22 (CDH 22) proteins were used as potential interferent biomolecules.

2.2. Apparatus and electrodes

IR analysis was performed by employing Bruker FTIR Vertex 70 spectrometer (Germany) in the range of 4000–400 cm^{-1}. The Raman analysis was performed by employing Thermo Scientific Raman-780 nm excitation laser (USA). ^1H NMR and ^{13}C NMR spectra of monomers and polymers were recorded by using 400 MHz Bruker Avance II (Bruker, Germany) employing $CDCl_3$ and DMSO-D_6. Electrochemical experiments were taken by Gamry Reference 1000 Workstation (USA). The ITO film (5 × 20 mm), the platinum wire and Ag/AgCl were used as working electrode, counter electrode and reference electrode, respectively. The surface morphology after modification was monitored by scanning electron microscopy with low vacuum detector, energy dispersive X-ray (QUANTA FEG-250, FEI, USA) and atomic force microscopy (tapping mode AFM, NanoMagnetics, Turkey). The scan rate of AFM was chosen as 2.5 μm/s with a resolution of 256 pixels per line. Three-dimensional AFM images were prepared with NanoMagnetics image analyzer software.

2.3. Synthesis of monomers and polymers

2.3.1. Synthesis of acid-substituted pyrrole monomer (Pyr-Pac)

The acid-substituted pyrrole monomer (*N*-Pyrrolylpropanoic acid) (Pyr-Pac) was synthesized according to the literature with minor modifications [39–41]. Acid substituted pyrrole monomer was obtained with conversion reaction of 1-(2-cyanoethyl) pyrrole as follows: 5 g (4.16 mmol) of N-1-(2-cyanoethyl) pyrrole was mixed with 30 mL potassium hydroxide solution (10 g, 17.8 mmol). The mixture was heated and stirred at 100 °C under a reflux of dry nitrogen for overnight. Then, the mixture was cooled to 25 °C and pH of mixture was arranged to 4 by dropping 8 M HCl solution. This mixture was extracted six times with diethyl ether (pH 4). At the end of this process, the organic layer was dried over anhydrous $MgSO_4$ and solvent was evaporated. Thus, pure product was produced as a beige crystalline.

(Yield: %82, 4.7 g). FTIR(ATR) cm^{-1}: 3500–3100; 2940–2884; 1695 (carbonyl); 1600–1450); 1216; 931; 787, 724; 647; 613; 500 (Fig. SI–2B). ^{1}H NMR (δ_H, ppm) (400 MHz, $CDCl_3$): 11.6 (Ha, 1H); 2.87 (Hb, 1H); 4.24 (Hc, 2H); 6.72 (Hd, 2H) and 6.20 (He, 2H) (Fig. SI-3). ^{13}C NMR (δ_C, ppm) (400 MHz, $CDCl_3$): 177.75 (a); 36.38 (b); 44.54 (c); 120.62 (d) and 108.66 (e) (Fig. SI-4).

2.3.2. Synthesis of methoxy-substituted pyrrole monomer (Pyr-Ome)

The methoxy-substituted pyrrole monomer (Pyr-Ome) was synthesized according to the literature with minor modifications [42,43]. Monomer (Pyr-Pac) (2.0 g, 0.014 mol) was solved in dry methanol (25 mL, ~25 equiv) in a flask charged with magnetic stirring bar and ten drops of concentrated H_2SO_4 was dropped and then, the solution was refluxed for 24 h under nitrogen. After 24 h, the solvent was evaporated and the remaining mixture was solved in diethyl ether and then, it was extracted with water (50 mL) four times. After that, the organic layer was dried over anhydrous $MgSO_4$ and filtered. Then, the solvent was evaporated to obtain a liquid monomer and then, it was purified by column chromatography.

(Yield: %92, 2.07 g) FTIR(ATR) cm^{-1}: 2990–2950; 1730(carbonyl); 1600–1450; 1221; 900; 775; 450(Fig. SI–2C). ^{1}H NMR (δ_H, ppm) (400 MHz, $CDCl_3$): 3.69 (Ha, 3H); 2.78 (Hb, 2H); 4.21 (Hc, 2H); 6.14 (Hd, 2H) and 6.67 (He, 2H) (Fig. SI-5). ^{13}C NMR (δ_C, ppm) (400 MHz, $CDCl_3$): 51.7 (a); 171.1 (b); 36.1 (c); 44.7 (d); 120.3 (e) and 108.2 (f) (Fig. SI-6).

2.3.3. Synthesis of acid-substituted pyrrole polymer (P(Pyr-Pac))

The conjugated polymer P(Pyr-Ome) was synthesized by chemical oxidative polymerization with anhydrous ferric chloride ($FeCl_3$), using Pyr-Ome as a monomer [44,45]. The monomer (Pyr-Ome) was dissolved in 15 mL of dry chloroform in a three-necked round bottom flask including a magnetic stirring bar and then, it was put in an ice-salt bath (−10/-15 °C) and argon inlet-outlet. Then, anhydrous ferric chloride ($FeCl_3$,2.12 g, 13.0 mmol) in 6 mL of nitromethane solution was added dropwise by using a syringe over 25 min. The mixture was stirred at room temperature under a flux of argon for 100 min. Total reaction time was 2 h. The obtained black polymer suspension was precipitated by using methanol (500 mL), and the black polymer was turned to brown. The precipitate was collected by filtration. To yield a pure polymer, it was rinsed with methanol (by employing a soxhlet) and with ultrapure water to eliminate the residual $FeCl_3$ and the oligomers. The polymer P (Pyr-Pac) was prepared by using a general hydrolyzation techniques in literature. The methyl groups on the polymer P(Pyr-Pac) side chain were removed by heating 0.2 g of the polymer in 10 mL of 2.0 M sodium hydroxide solution for 24 h at 100 °C. Then, the mixture was filtered to eliminate the insoluble part. Then, water soluble fraction was acidified with a solution of concentrated HCl and it was filtered. The solid polymer was rinsed repeatedly with ultrapure water and dried under vacuum in two days.

(Yield: %48, 90 mg). FTIR(ATR) cm^{-1}: 2950–2926 (CH); 1705 (C═O); 1592, 1420(C═C); 1184; 900; 776; 605(Fig. SI-2E). ^{1}H NMR (δ_H, ppm) (400 MHz, DMSO-D_6): 6.81 ppm (Ha), 4.20 ppm (Hb) ve 2.92 ppm (Hc) (Fig. SI-7).

2.4. Procedures

2.4.1. Preparation of CCR4 immunosensor

Firstly, ITO electrodes successively washed in ultrasonic cleaner with acetone, soap solution and ultrapure water. After that, the ITO electrodes were hydroxylated by dipping into the fresh mixed solution (H_2O: NH_4OH:H_2O_2 = 5:1:1) for 90 min, washed with ultrapure water, and dried using argon flow. In order to form self-assembled polymer monolayers on the hydroxylated ITO electrodes, they were immersed into P(Pyr-Pac) polymer solution to form ester bond [46]. After that, the obtained ITO sheets were washed with ultrapure water thoroughly and dried under flowing argon. The immobilization of the anti-CCR4 antibodies was achieved using to chemical agents, a coupling reagent (NHS) and crosslinking reagent (EDC). Because of this, ITO electrodes were incubated in NHS (0.01 M)/EDC (0.04 M) to activate the carboxyl groups. Then, ITO electrodes were immersed into anti-CCR4 antibody solution and incubated there 45 min, rinsed thoroughly with ultrapure water to eliminate unbounded anti-CCR4 antibodies. At the next step of modification, the electrodes were then immersed in BSA solution for 1 h and BSA molecules were blocking agents for free carboxyl ends. After washing and drying, the CCR4 antigen specific electrochemical biosensing platform was prepared.

2.4.2. Electrochemical detection of CCR4 antigen

In this study, $[Fe(CN)_6]^{4-/3-}$ was utilized as a redox probe and it was prepared by using 1 M KCl and 5 mM $K_3Fe(CN)_6/K_4Fe(CN)_6$ (1:1). The CV potential was from −0.5 to 1 V at a scan rate of 100 mV/s. The EIS frequency was from 50 kHz to 0.5 Hz CCR4 determination was performed by utilizing ITO/P(Pyr-Pac)/NHS-EDC/anti-CCR4/BSA/CCR4 electrode.

2.4.3. Determination of CCR_4 antigen

The CCR4 antigen was determined using the ITO/P(Pyr-Pac)/NHS-EDC/anti-CCR4/BSA immunoelectrode as a working electrode. Firstly, these immunoelectrodes were immersed in PBS solution including different levels of CCR4 antigen. After that, EIS analyses were recorded. The relationship between EIS response and CCR4 antigen concentration was used for quantification of CCR4 antigen.

3. Results and discussion

Pyrrole polymer (P(Pyr-Pac) containing the acid side groups was successfully synthesized by using a several reaction stages. The reaction stages included conversion (nitrile to acid), esterification, polymerization and hydrolyzation methods. Firstly, 1-(2-cyanoethyl)pyrrole was converted to the *N*-pyrrolylpropanoic acid monomer (Pyr-Pac) by the addition of potassium hydroxide. Secondly, methyl 3-(1H-pyrrol-1-yl) propanoate (Pyr-Ome) was synthesizeded by a reaction of *N*-pyrrolylpropanoic acid in dry methanol including a small amount of concentrated H_2SO_4. This polymerization technique was selected instead of the direct polymerization of *N*-pyrrolylpropanoic acid (Pyr-Pac) since the carboxylic acid group interfered with the $FeCl_3$ polymerization. Thirdly, the 3-(1H-pyrrol-1-yl)propanoate monomer (Pyr-Ome) was polymerized via chemical oxidative coupling technique to produce a polymer with methyl side groups P(Pyr-Ome). Fourthly, the polymer P(Pyr-Ome) was hydrolyzed to synthesize the polymer P(Pyr-Pac) containing acid side groups by heating the polymer in 2.0 M sodium hydroxide aqueous solution for 24 h at 100 ^{O}C. Lastly, the polymer was neutralized by dilute hydrochloric acid solution to obtain polymer P(Pyr-Pac). Additionally, the procedures for preparation of monomer and polymers, and the chemical structure characterization of polymers are given in supp. material part.

Scheme 1 shows the modification stages implied in the fabrication of the ITO/P(Pyr-Pac)/NHS-EDC/anti-CCR4/BSA/CCR4 immunosensor. The fabrication process included 4 stages; modification of disposable ITO electrode by polymer P(Pyr-Pac) (step 1), activation of free carboxyl groups with NHS/EDC coupling (step 2), covalent immobilization of anti-CCR4 antibodies on the ITO/P(Pyr-Pac) surface (step 3), blockage the free carboxyl ends via BSA solution (step 4) and determination of CCR4 antigens (step 5).

3.1. Chemical characterizations of P(Pyr-Pac) modified and anti-CCR4 attached ITO electrode surfaces

The infrared spectra of the polymer P(Pyr-Pac) modified ITO electrode (purple line) and anti-CCR4 modified ITO (red line) are showed in Fig. 1A, B, respectively. As seen in Fig. 1A, the acid-substituted pyrrole polymer self-assembled ITO substrate had small broad absorption peak at 1725 cm^{-1} that confirmed the ester bond between polymer P(Pyr-

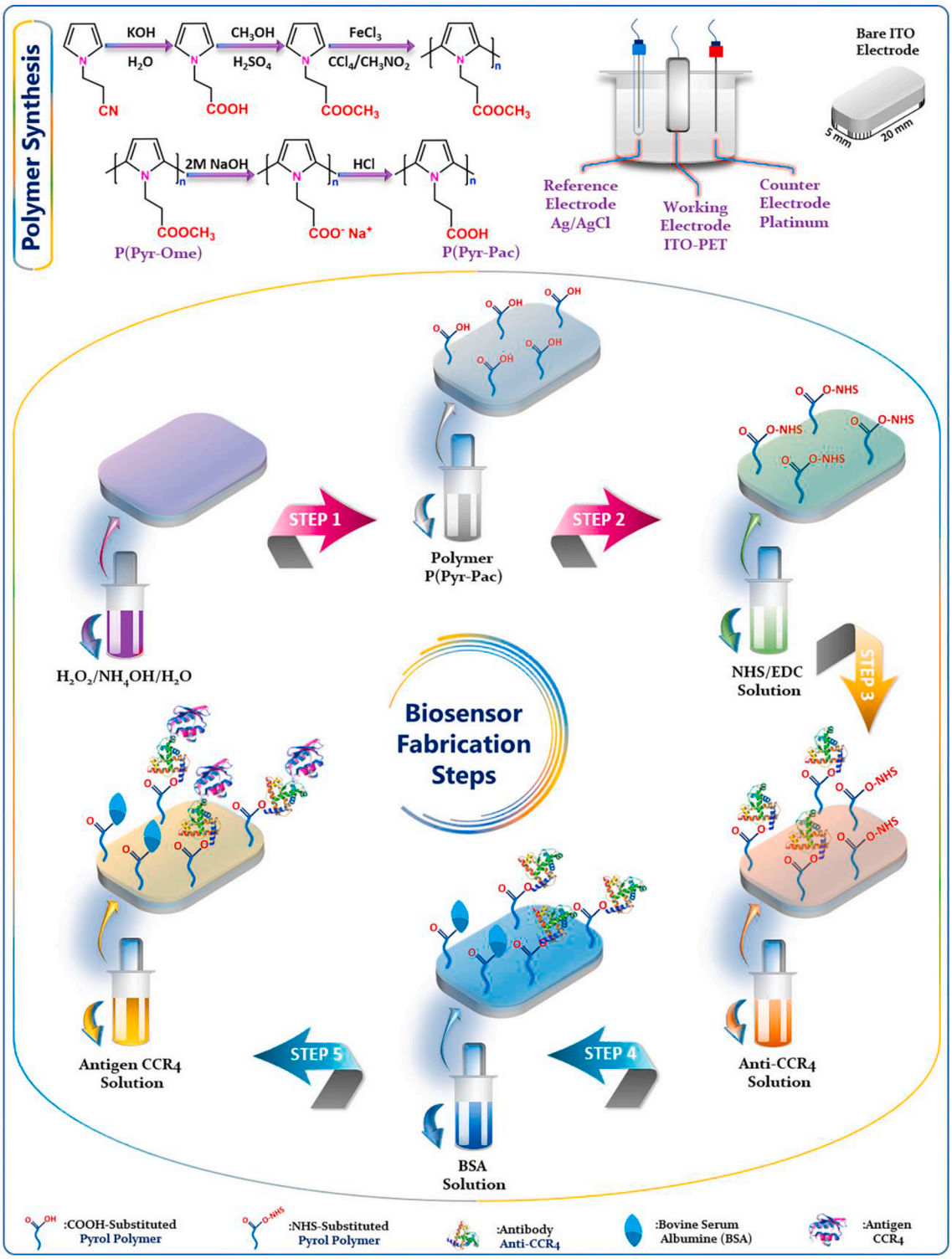

Scheme 1. Synthesis steps of P(Pyr-Pac) polymer used for immunosensor development and construction procedure of the designed CCR4 biosensor.

Pac) and hydroxyl groups present on ITO substrate [21,47]. The strong signal appeared around 1690 cm^{-1} was originated from C═O stretching vibration of acid side groups in P(Pyr-Pac) polymer [48]. Furthermore, the broad band between 3200 and 3600 cm^{-1} proved the –OH bonds of side groups in polymer [39]. Fig. 1B exhibits the FTIR spectrum of ITO/P (Pyr-Pac)/anti-CCR4 antibody electrode. At red line in Fig. 1B, the broad and intense bands at around 1650 cm^{-1}(amid I) and 1553 cm^{-1} (amid II) were classical protein bands, and this band showed the attachment of the anti-CCR4 antibody to polymer P(Pyr-Pac) self-assembled ITO surface [49–51]. Apart from FTIR analysis, the chemical characterization of polymer self-assembled ITO electrode surface (purple line) and anti-CCR4 antibody immobilized ITO surface (red line) were carried out via Raman spectroscopy (Fig. 1C, D). Raman spectroscopy techniqu was utilized to investigate the formation of the bonds on the ITO substrate surface during biosensor fabrication [52–54]. At purple line in Fig. 1C, polymer self-assembled ITO substrate surface, had peaks like FTIR

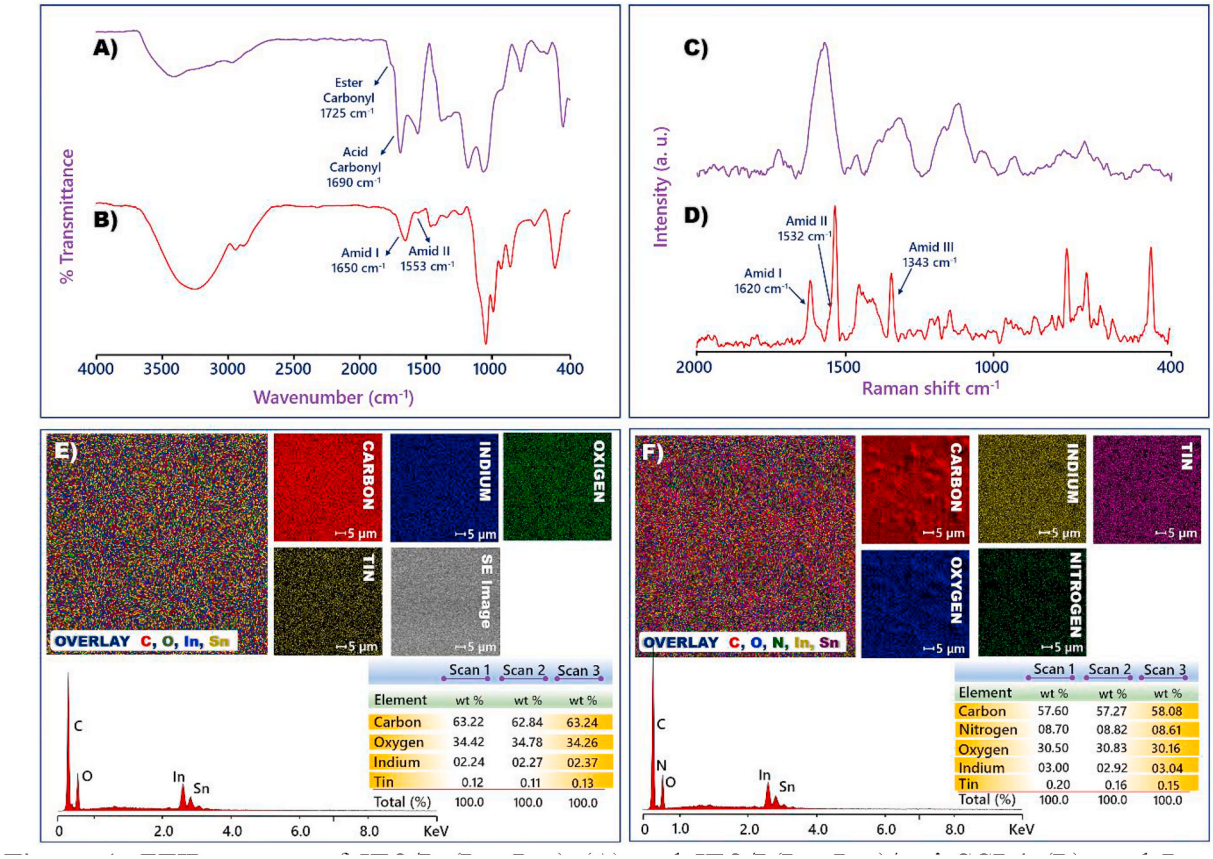

Fig. 1. FTIR spectra of ITO/P (Pyr-Pac) (A) and ITO/P(Pyr-Pac)/anti-CCR4 (B); and Raman spectra of ITO/P(Pyr-Pac) (C) and ITO/P(Pyr-Pac)/anti-CCR4 (D); EDX analysis results of bare ITO (E) and ITO/P (Pyr-Pac) (F).

spectrum. The Raman spectroscopy measurement is more proper way to monitor amide bonds than FTIR measurement [55]. The bands of amide I, II and III regions are observed between 1600 and 1680 cm^{-1}, 1480-1570 cm^{-1} and 1235-1350 cm^{-1}, respectively [56,57]. As illustrated in Fig. 1D, amide I, amide II and amide III bonds were found at 1620, 1532 and 1343 cm^{-1}, respectively [58].

Moreover, energy dispersive X-ray spectroscopy (EDX) measurement was taken from the bare ITO electrode surface and P(Pyr-Pac) polymer modified surface. The elemental distribution of bare ITO electrode illustrated high percentages of carbon, oxygen, indium and tin, which originated from the nature of ITO electrode. The elemental distribution of P(Pyr-Pac) modified ITO surface contained the nitrogen element, unlike the bare electrode. The nitrogen element originated from the polymer chain of P(Pyr-Pac). The ratios of nitrogen element from different areas on the same ITO surface were 8.70%, 8.82% and 8.61%. The closeness of the ratios to each other displayed the presence of homogenous polymer matrix on the ITO substrate surface.

3.2. *Electrochemical characterization of the designed CCR4 biosensor fabrication steps*

The electrochemical impedance spectra of the CCR4 immunosensor layer-by-layer modification steps were investigated in the presence of redox couple $[Fe(CN)_6]^{3-/4-}$. Nyquist plots after sequential modification

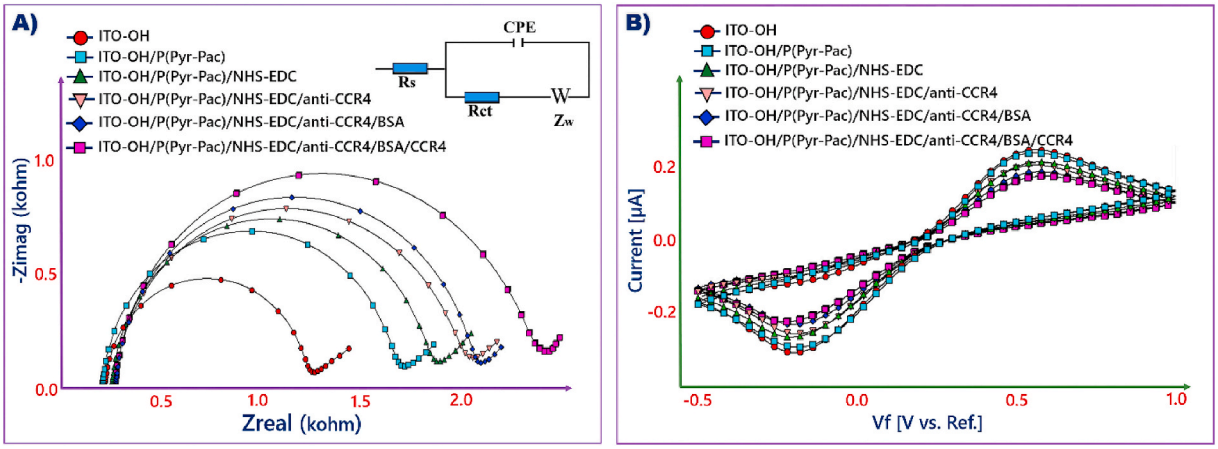

Fig. 2. Electrochemical impedance spectra (A) and Cyclic voltammograms (B) of CCR4 immunosensor construction steps.

of polymer P(Pyr-Pac), anti-CCR4 antibody, BSA and CCR4 antigen on the ITO surface are displayed in Fig. 2A. Each Nyquist plot includes a partial semicircle at high frequency part and a straight line at low frequency part. Fig. 2A clearly demonstrated that the semicircle diameter increases because of increasing difficulties in electron transfer after more and more biomolecules immobilization on the ITO electrode surface. To evaluate the EIS spectra, a Randles equivalent circuit (Fig. 2A inset) was utilized to fit the impedance data. Randles equivalent circuit includes the electrolyte solution resistance (R_s), the charge transfer resistance (R_{ct}), the constant phase element (CPE) and Warburg impedance (W) [59,60]. As displayed in Fig. 2A, hydroxylated ITO electrode had the minimum electron transfer resistances (R_{ct}). After polymer P(Pyr-Pac) modification on the ITO surface, the semicircle part of the Nyquist plot illustrated an increase in the diameter. In this circumstance, the electron transfer was decreased due to polymer coating and therefore, the diameter of semicircle of Nyquist plot increased. After activation of carboxyl groups of polymer P(Pyr-Pac), the R_{ct} increased because of the charge repulsion between redox probe and negative carboxyl groups. Thus, the electron transfer rate reduced. After coupling anti-CCR4 antibody on the ITO electrode surface, the amount of R_{ct} increased much more. By reason of the attachment of anti-CCR4 antibodies on the ITO surface, the electron transfer was prevented. Then, BSA was utilized to eliminate non-specific binding and because of this, an increase was observed in R_{ct}. The R_{ct} increased while CCR4 antigen was cast on the ITO substrate. Also, ITO/P(Pyr-Pac)/NHS-EDC/anti-CCR4/BSA/CCR4 electrode illustrated the highest resistance among others. This increase proved the immobilization of biomolecules on the ITO electrode. As presented in Fig. 2B, the CV of the hydroxylated ITO electrode had maximum peak currents. Self-assembling of P(Pyr-Pac) polymer and immobilization of anti-CCR4, BSA and CCR4 antigen caused decreases in oxidation and reduction CV peaks. The ITO/P(Pyr-Pac)/NHS-EDC/anti-CCR4/BSA/CCR4 illustrated the lowest peak currents as compared to other modification stages of the ITO electrode. These decreased might be originated from several proteins' immobilization on the ITO electrode surface. Thus, the ITO-based biosensor fabrication stages were performed successfully.

3.3. Morphological characterization of the modified electrode surfaces

Fig. 3Aand B shows the SEM and AFM images of bare ITO electrode. The average roughness of bare ITO electrode surface was 0.4 nm. At the hydroxylated ITO electrode (Fig. 3C, D), the surface of the ITO electrode looked like bare ITO surface and the average roughness (R_a) of ITO/OH electrode was 1 nm. Fig. 3E, F displays the SEM and AFM images of polymer functionalized ITO substrate surface and a homogenous polymer layer self-assembled on the ITO electrode surface. The average roughness of the polymer self-assembled ITO sheet was 31.5 nm. This increase in R_a proved that a polymer self-assembled monolayer was formed successfully. Anti-CCR4 antibodies exhibited sphere-like structure and an uneven surface (Fig. 3G). The average roughness of the antibody immobilized ITO surface was 31.9 nm (Fig. 3H). After BSA blockage step, the surface morphology was changed significantly (Fig. 3I, J) and a decrease was observed in R_a value (29.6 nm) owing to

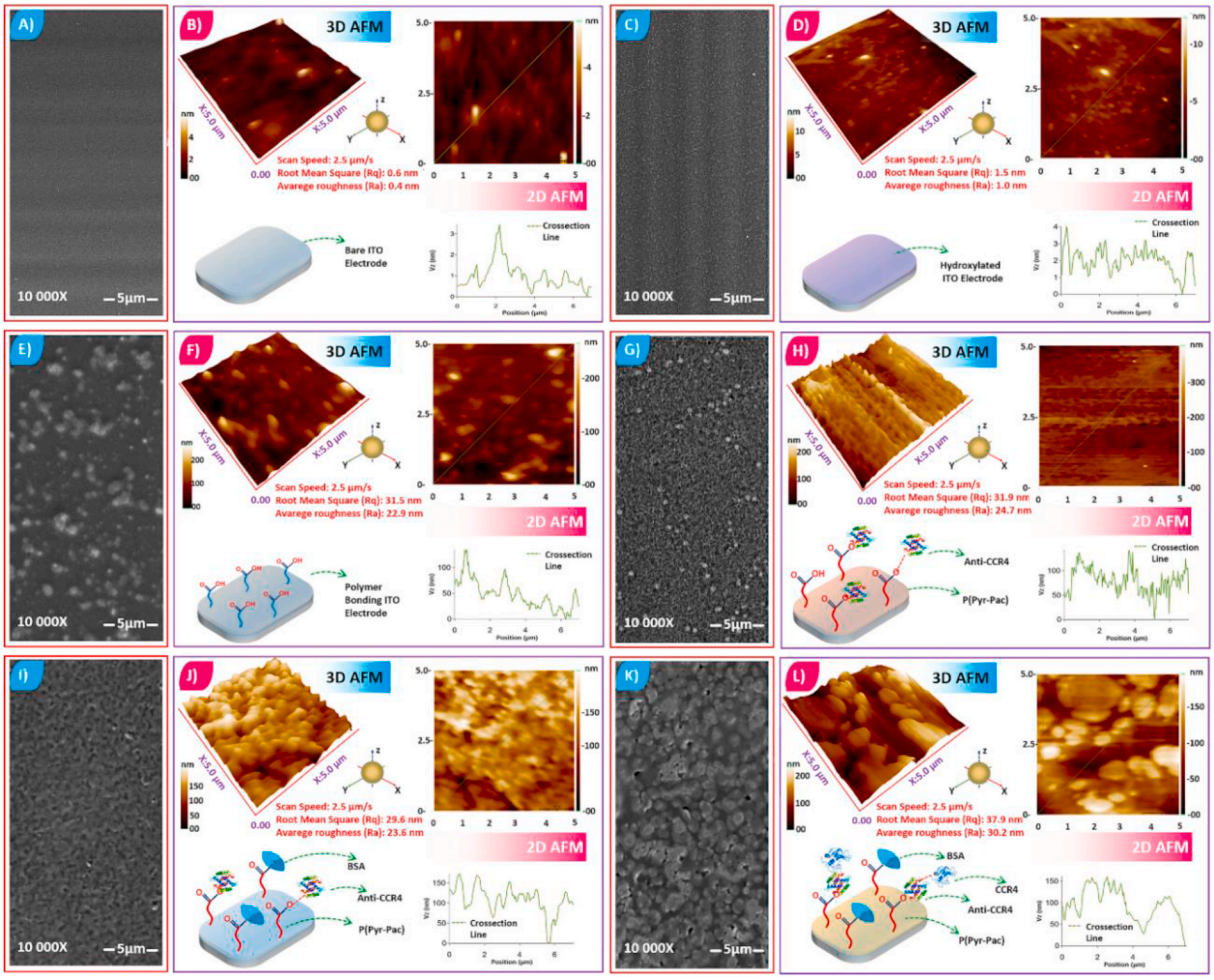

Fig. 3. SEM and AFM images of bare ITO (A and B), ITO/OH (C and D), ITO/P(Pyr-Pac) (E and F), ITO/P(Pyr-Pac)/anti-CCR4 (G and H), ITO/P(Pyr-Pac)/anti-CCR4/BSA (I and J), ITO/P(Pyr-Pac)/anti-CCR4/BSA/CCR4 (K and L).

smooth surface formation. After immobilization of CCR4 antigen, the surface morphology varied significantly. As monitored in Fig. 3K, L, CCR4 antigen macro-biomolecules were present on the working electrode surface. The R_a of the CCR4 antigen attached ITO electrode was 30.2 nm and this increase clearly confirmed specific interaction between anti-CCR4 antibodies and CCR4 antigens.

3.4. Experimental parameters optimization

To obtain best performance of the CCR4 biosensor, four experimental conditions including polymer concentration, anti-CCR4 antibody level and anti-CCR4 antibody incubation duration, CCR4 antigen incubation duration were optimized before analytical studies. While the optimization of one parameter, other parameters were kept constant, and all experiments were performed at room temperature. The results of the experimental conditions are displayed in Fig. 4.

First, the amount of polymer used in the CCR4 biosensor construction process was optimized. Fig. 4A shows the impedimetric response of the immunosensor which fabricated by using various concentration of polymer (0.125 mg/mL, 0.5 mg/mL and 1 mg/mL). As displayed in Fig. 4A, the impedimetric response did not increased with increasing the polymer concentration from 0.125 mg/mL to 1 mg/mL. Because of this, 0.125 mg/mL was selected as the optimum polymer amount. Thereafter, the influence of antibody level on the biosensor signal was studied. Based on Fig. 4B, with increasing the antibody level, the biosensor signal was increased. When used anti-CCR4 antibody concentration was 4 ng/mL, the impedimetric signal was low. Hence, 2 ng/mL was selected as optimum antibody concentration. The anti-CCR4 antibody incubation time to cover the carboxyl ends of polymer influenced the biosensor response. Because of this, the ITO/P(Pyr-Pac) electrodes were dipped in antibody solution for three different durations and employed for CCR4 determination. After 45 min, there was not obvious change on the EIS response as displayed in Fig. 4C. Thus, 45 min was selected as the optimum antibody incubation time (Fig. 4C). The antibody and antigen interaction times were another essential parameters during the biosensor fabrication. The ITO/P(Pyr-Pac)/anti-CCR4/BSA electrodes were dipped into CCR4 antigen solution for various duration (30 min, 45 min and 60 min). The maximum biosensor response was measured after 30 min incubation. Because of this reason, 30 min was enough for CCR4 antigen concentration determination and the short incubation time is important for practicality of the designed biosensor (Fig. 4D).

3.5. Analytical performance of the designed biosensor for quantification of CCR4

The electrochemical behavior of the designed biosensor incubated with different CCR4 antigen levels were investigated by EIS and CV. Fig. 5A, B shows the EIS spectra and CVs after attachment of different levels of CCR4 from 0.02 to 8 pg/mL. Under the optimum conditions, the impedance values increased, and current values decreased as CCR4 concentration increased. The impedimetric signals of the immunosensor were linearly proportional to the CCR4 antigen concentration and this system exhibited concentration-dependent response. A linear detection range of 0.02–8 pg/mL ($R^2 = 0.997$) was observed for CCR4 antigen and the limit of detection (LOD) was found as 6.4 fg/mL based on 3 sb/m. The limit of quantification (LOQ, 10 sb/m) and sensitivity were calculated as 21.4 fg/mL and 2.07 kΩ pg^{-1} $mLcm^{-2}$, respectively (sb/m; the standard deviation of 5 impedimetric signals recorded without CCR4 antigen, and n was the slope of the calibration curve). Since this was the first immunosensor fabricated so far for CCR4 detection, its analytical features could only be compared to commercial ELISA kit. The ELISA kit had higher LOD (46.875 pg/mL) than our immunosensor. Additionally, the designed immunosensor could determine the CCR4 level in shorter time than conventional ELISA. Furthermore, the immunosensor had

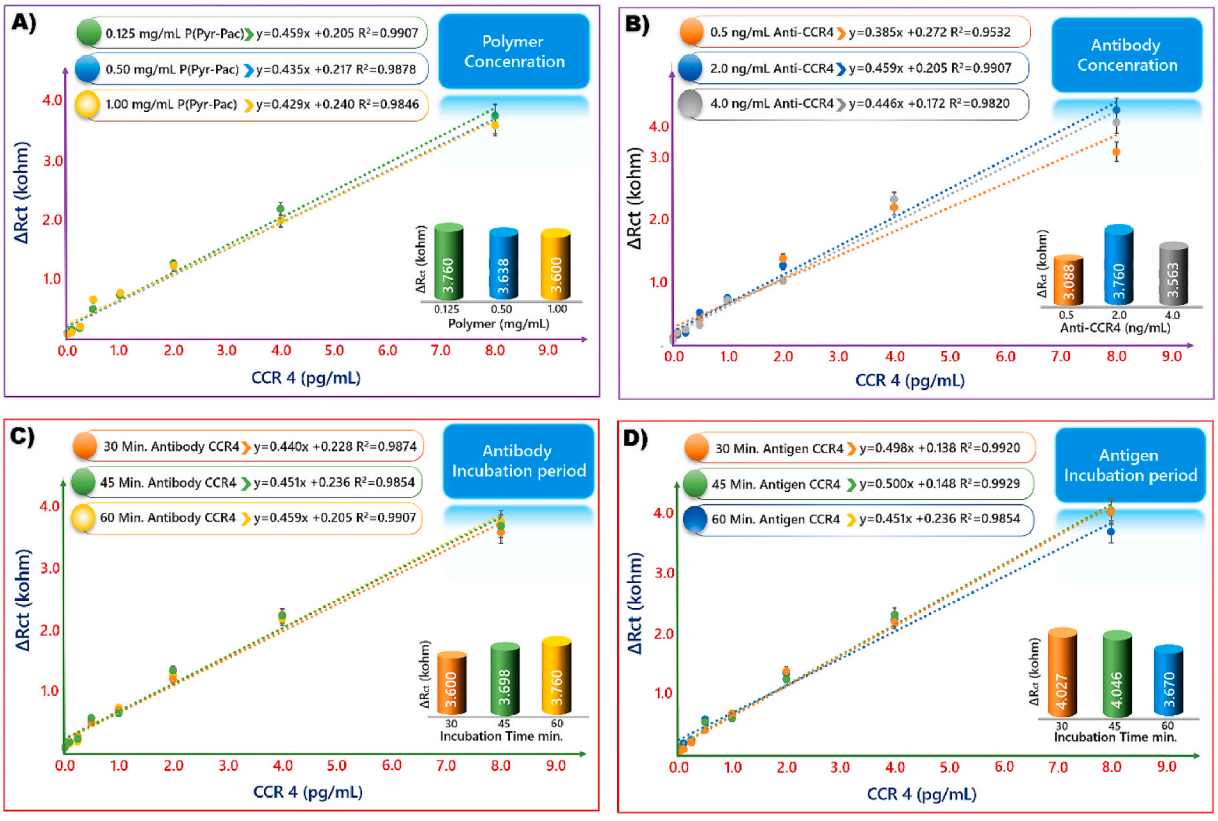

Fig. 4. Results of optimization studies; P(Pyr-Pac) polymer amount (A), anti-CCR4 antibody level (B), anti-CCR4 antibody incubation time (C), CCR4 antigen incubation time (D).

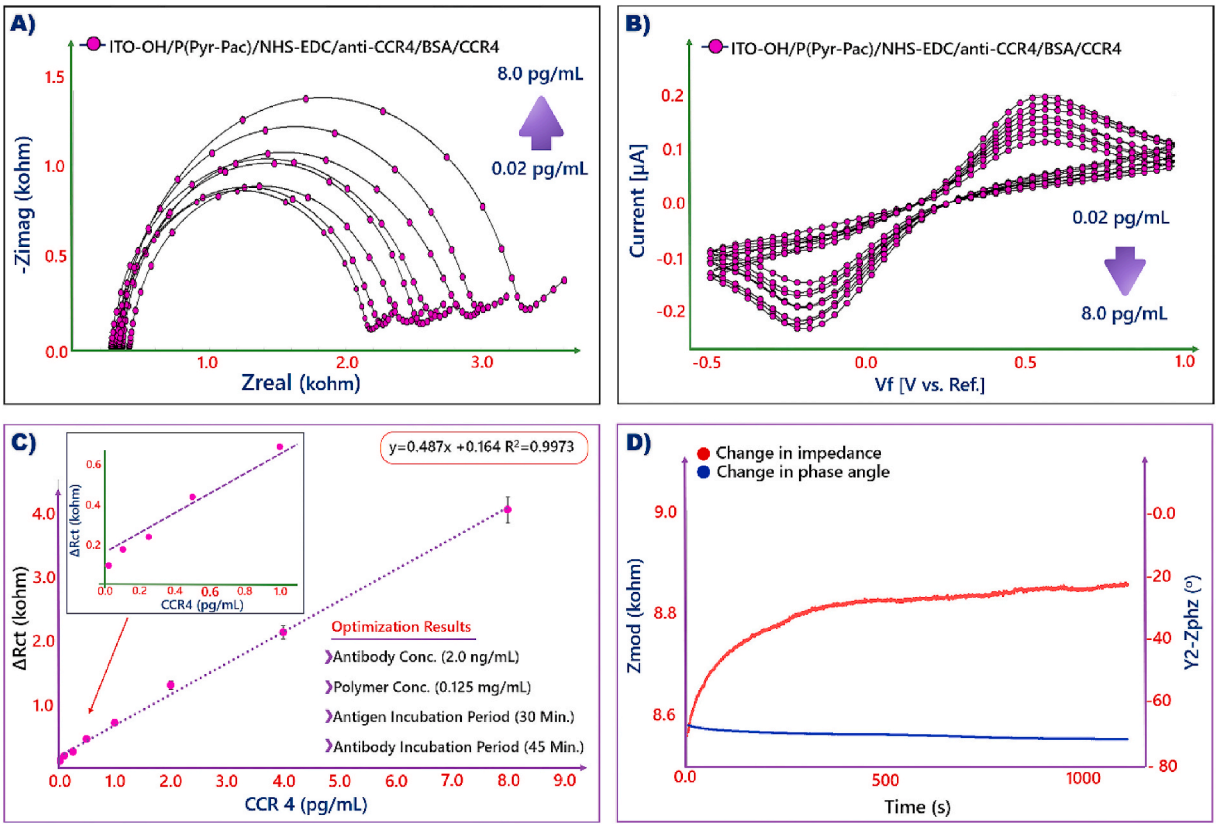

Fig. 5. Nyquist plots (A) and CVs (B) of the suggested biosensor with increases in CCR4 antigen concentration from 0.02 to 8 pg/mL, the calibration plot (C) and SFI result of the proposed system (D).

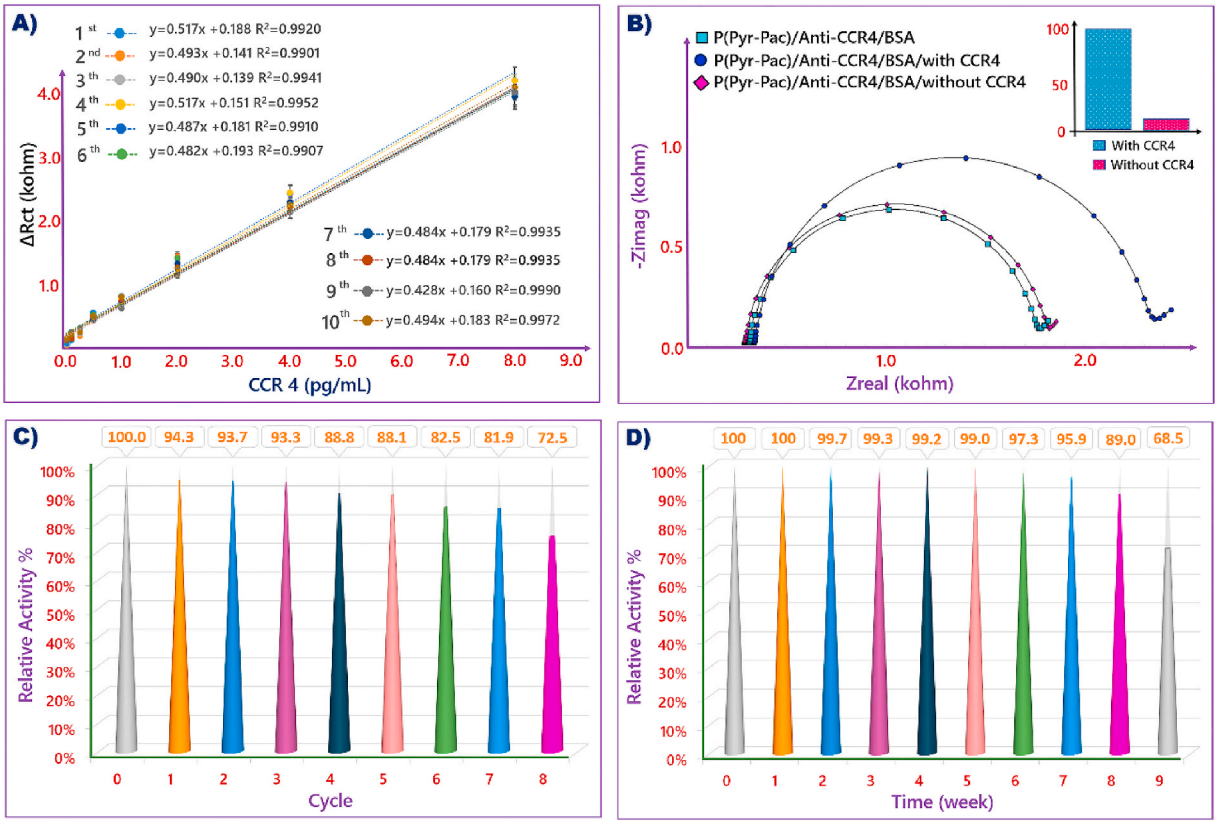

Fig. 6. Results of reproducibility (A), selectivity test performed with interference biomarkers and CCR4 antigen (B), regeneration (C) and storage stability (D).

portable and low-cost device, which made it an ideal tool for routine analyses of biomarkers.

In addition to EIS and CV electrochemical techniques, a different approach of single frequency analysis was performed to investigate the biomolecular sensing. In this system, the interaction between antibody and antigen was analyzed at fixed frequency [44,45]. Fig. 5D shows the SFI spectra of the proposed CCR4 biosensor in PBS containing CCR4 antigen. The fixed frequency was determined by using Bode Plot and used in the SFI experiment. As seen in Fig. 5D, an increase was seen in impedance signal. This increase proved the specific bio-interaction.

3.6. Repeatability, reproducibility, selectivity, regeneration and shelf-life of the proposed biosensor

Repeatability and reproducibility are two effective features to illustrate the performance of the immunosensor. For this reason, the repeatability and reproducibility of the immunosensor were investigated. In order to evaluate repeatability of the system, 20 different electrode surfaces fabricated on the same day were employed to detect CCR4 antigen at the same concentration (1 pg/mL). The relative standard deviation (RSD) of the measurements was 5.13%. The result displayed that the immunosensor had good repeatability. In order to test the reproducibility, 10 different biosensors constructed at the same experimental conditions were used for reproducibility test and the RSD value was found as 2.66%, which displayed the good reproducibility of the immunosensor construction procedure and the impedimetric determination (Fig. 6A).

Furthermore, in order to analyze the selectivity of the designed biosensor, the two different ITO/P(Pyr-Pac)/anti-CCR4/BSA electrodes were prepared and one of them was dipped in PBS solution containing interferent biomarkers (MAGE 1, PAK 2, CDH 22) and the other was dipped in PBS solution containing all biomarkers (MAGE 1, PAK2, CDH22 and CCR4). The interferent biomarkers concentrations were 100 times higher than CCR4 antigen concentration. Fig. 6B shows EIS spectra of the immunosensors incubated in these solutions. As expected, impedimetric response of the second one was higher than the first one, which illustrated that the proposed immunosensor had high selectivity to CCR4 antigen (Fig. 6B).

The regeneration of a biosensor is important in practical applications. To examine whether the proposed immunosensor can be reused, the ITO surface attached with CCR4 antigen (ITO/P(Pyr-Pac)/anti-CCR4/BSA/CCR4) was dipped in HCl solution (10 mM) for 5 min. Then, the response of the immunosensor was measured. After that, it was incubated in CCR4 antigen solution and after 30 min-incubation, the electrochemical response was measured. As seen in Fig. 6C, after acidic treatment, impedimetric responses were diminished obviously. The designed biosensor could be reused at least 8 times, and the impedimetric response decreased to 72.5% of the initial signal (Fig. 6C).

At the same time, the storage-stability of the suggested immunosensor was investigated. Ten different ITO/P(Pyr-Pac)/anti-CCR4/BSA electrodes were firstly stored at 4 °C and each week, one of these electrodes was immersed in PBS solution containing CCR4 antigen and then, examined by EIS after specific interaction with CCR4 antigen. Experiments illustrated that the proposed immunosensor retained 68.5% of its initial signal after 9 weeks (Fig. 6D).

3.7. Determination of CCR4 antigen in human serum samples

To analyze the usability of the suggested immunosensor for CCR4 antigen concentration determination, 5 different serum samples were supplied from Tekirdağ Namık Kemal University Hospital. CCR4 antigen detection was performed after simple dilution with PBS buffer (200-fold). The accuracy of the sensing technique was verified by standard addition method. As listed in Table 1, the recovery rates for CCR4 antigen in human serum were from 98.25% to 103.99%. These results exhibited good accuracy for the P(Pyr-Pac) based immunosensor in human serum samples for CCR4 antigen detection, indicating a great potential in real samples analyses. Moreover, the proposed biosensor ($0.05 per test) was able to measure the CCR4 biomarker concentration less costly than ELISA kit ($8.54 per test). The proposed immunosensor was attractive and user-friendly way to detect CCR4 serum levels and this technique was more suitable than ELISA technique.

4. Conclusion

This study reported the first biosensor for the impedimetric determination of CCR4, a biomarker of prostate cancer. In this design, P(Pyr-Pac) modified ITO sheet was used as biosensing element immobilization material and anti-CCR4 antibodies were used as biorecognition elements. The proposed immunosensor was developed by immobilizing of anti-CCR4 antibodies on the ITO/P(Pyr-Pac) electrode through NHS/EDC chemistry. The amount of polymer (Pyr-Pac) and anti-CCR4 antibody immobilized, immobilization times of anti-CCR4 antibody and CCR4 antigen were also optimized. The proposed electrochemical immunosensor could sensitively detect CCR4 antigen in a range from 0.02 to 8 pg/mL with a detection limit of 6.4 fg/mL, which was lower than conventional ELISA. It also exhibited good selectivity and acceptable reproducibility for CCR4 antigen detection. Moreover, the suggested immunosensor had promising potential for CCR4 antigen detection in human serum samples. Additionally, the suggested immunosensor displayed satisfactory stability. After long-term storage (4 °C in dry form), 89.0% (eight weeks) of the initial signal was preserved, illustrating the designed immunosensor could be employed for CCR4 antigen measurement with acceptable stability. Thus, all the results described in this work shows the potential of the suggested immunosensor for determination of cancer biomarkers.

Table 1
Determination of CCR4 antigen in human serum samples.

Sample	Found by biosensor (pg/mL)	Added CCR 4 antigen (pg/mL)	*SD and *CV (%)	Total found by biosensor	*SD and *CV (%)	Recovery (%)	Relative difference (%)
1	1.10	0.5	0.05, 4.23	1.57	0.07, 4.30	98.23	−1.75
1	1.17	0.5		1.67		100.16	0.16
2	1.05	0.5	0.04, 4.04	1.62	0.01, 0.54	104.55	4.55
2	1.11	0.5		1.63		101.32	1.32
3	2.04	0.5	0.08, 3.87	2.64	0.02, 0.71	103.99	3.99
3	2.16	0.5		2.67		100.49	0.49
4	0.79	0.5	0.04, 4.63	1.29	0.03, 2.53	100.37	0.37
4	0.84	0.5		1.34		99.9	−0.10
5	1.91	0.5	0.02, 1.13	2.43	0.03, 1.07	100.80	0.80
5	1.94	0.5		2.47		98.23	−1.75

*SD: Standard Deviation, *CV: Coefficient Variation.

Credit author statement

Elif Burcu Aydın: biosensor fabrication, electrochemical measurements, software, writing. Muhammet Aydın: Monomer synthesis, polymer synthesis, chemical characterization, morphological characterization, morphological measurements, software. Mustafa Kemal Sezginturk: Biosensor fabrication, electrochemical measurements, writing.

Declaration of competing interest

The authors declare that they have no known competing financial interests or personal relationships that could have appeared to influence the work reported in this paper.

Acknowledgement

This research was supported The Scientific and Technological Research Council of by Çanakkale Onsekiz Mart University, ÇOMÜ-BAP (Grant number: FUK-2018-1396).

Appendix A. Supplementary data

Supplementary data to this article can be found online at https://doi.org/10.1016/j.talanta.2020.121487.

References

[1] F.H. Schröder, J. Hugosson, M.J. Roobol, T.L. Tammela, S. Ciatto, V. Nelen, M. Kwiatkowski, M. Lujan, H. Lilja, M. Zappa, Screening and prostate-cancer mortality in a randomized European study, N. Engl. J. Med. 360 (13) (2009) 1320–1328.
[2] P.S. Mitchell, R.K. Parkin, E.M. Kroh, B.R. Fritz, S.K. Wyman, E.L. Pogosova-Agadjanyan, A. Peterson, J. Noteboom, K.C. O'Briant, A. Allen, Circulating microRNAs as stable blood-based markers for cancer detection, Proc. Natl. Acad. Sci. Unit. States Am. 105 (30) (2008) 10513–10518.
[3] S. Singh, A.A. Gill, M. Nlooto, R. Karpoormath, Prostate Cancer Biomarkers Detection Using Nanoparticles Based Electrochemical Biosensors, Biosensors and Bioelectronics, 2019.
[4] L.-H. Pan, S.-H. Kuo, T.-Y. Lin, C.-W. Lin, P.-Y. Fang, H.-W. Yang, An electrochemical biosensor to simultaneously detect VEGF and PSA for early prostate cancer diagnosis based on graphene oxide/ssDNA/PLLA nanoparticles, Biosens. Bioelectron. 89 (2017) 598–605.
[5] L.F. Cheow, S.H. Ko, S.J. Kim, K.H. Kang, J. Han, Increasing the sensitivity of enzyme-linked immunosorbent assay using multiplexed electrokinetic concentrator, Anal. Chem. 82 (8) (2010) 3383–3388.
[6] E. Tonutti, D. Bassetti, A. Piazza, D. Visentini, M. Poletto, F. Bassetto, P. Caciagli, D. Villalta, R. Tozzoli, N. Bizzaro, Diagnostic accuracy of ELISA methods as an alternative screening test to indirect immunofluorescence for the detection of antinuclear antibodies. Evaluation of five commercial kits, Autoimmunity 37 (2) (2004) 171–176.
[7] S. Ushaa, M. Madhavilatha, G.M. Rao, Design and analysis of nanowire sensor array for prostate cancer detection, Int. J. Nano Biomaterials (IJNBM) 3 (3) (2011) 239–255.
[8] C. Stephan, H. Cammann, H.-A. Meyer, M. Lein, K. Jung, PSA and new biomarkers within multivariate models to improve early detection of prostate cancer, Canc. Lett. 249 (1) (2007) 18–29.
[9] D.P. Ankerst, I.M. Thompson, Sensitivity and specificity of prostate-specific antigen for prostate cancer detection with high rates of biopsy verification, Archivio italiano di urologia, andrologia: organo ufficiale [di] Societa italiana di ecografia urologica, e nefrologica 78 (4) (2006) 125–129.
[10] M.M. Siddiqui, S. Rais-Bahrami, H. Truong, L. Stamatakis, S. Vourganti, J. Nix, A. N. Hoang, A. Walton-Diaz, B. Shuch, M. Weintraub, Magnetic resonance imaging/ultrasound–fusion biopsy significantly upgrades prostate cancer versus systematic 12-core transrectal ultrasound biopsy, Eur. Urol. 64 (5) (2013) 713–719.
[11] M. Remer, A. Al-Shamkhani, M. Glennie, P. Johnson, Mogamulizumab and the treatment of CCR4-positive T-cell lymphomas, Immunotherapy 6 (11) (2014) 1187–1206.
[12] Q. Liu, M. Rexiati, Y. Yang, W.-G. Wang, B. Azhati, W. SaiMaiti, Y.-J. Wang, Expression of chemokine receptor 4 was associated with poor survival in renal cell carcinoma, Med. Oncol. 31 (4) (2014) 882.
[13] T. Ishida, R. Ueda, CCR4 as a novel molecular target for immunotherapy of cancer, Canc. Sci. 97 (11) (2006) 1139–1146.
[14] R. Solari, J.E. Pease, Targeting chemokine receptors in disease–a case study of CCR4, Eur. J. Pharmacol. 763 (2015) 169–177.
[15] M. Locati, Massimo, M. Murphy, M. Philip, Chemokines and chemokine receptors: biology and clinical relevance in inflammation and AIDS, Annu. Rev. Med. 50 (1) (1999) 425–440.
[16] M. Vela, M. Aris, M. Llorente, J.A. Garcia-Sanz, L. Kremer, Chemokine receptor-specific antibodies in cancer immunotherapy: achievements and challenges, Front. Immunol. 6 (2015) 12.
[17] A. Ben-Baruch, Organ selectivity in metastasis: regulation by chemokines and their receptors, Clin. Exp. Metastasis 25 (4) (2008) 345–356.
[18] M. Wakugawa, K. Nakamura, T. Kakinuma, K. Tamaki, N. Onai, K. Matsushima, CC chemokine receptor 4 expression on peripheral blood CD4+ T cells reflects disease activity of atopic dermatitis, J. Invest. Dermatol. 117 (2) (2001) 188–196.
[19] A. Maolake, K. Izumi, K. Shigehara, A. Natsagdorj, H. Iwamoto, S. Kadomoto, Y. Takezawa, K. Machioka, K. Narimoto, M. Namiki, Tumor-associated macrophages promote prostate cancer migration through activation of the CCL22–CCR4 axis, Oncotarget 8 (6) (2017) 9739.
[20] E.B. Aydın, M. Aydın, M.K. Sezgintürk, Selective and ultrasensitive electrochemical immunosensing of NSE cancer biomarker in human serum using epoxy-substituted poly (pyrrole) polymer modified disposable ITO electrode, Sensor. Actuator. B Chem. 306 (2020) 127613.
[21] M. Aydın, E.B. Aydın, M.K. Sezgintürk, A disposable immunosensor using ITO based electrode modified by a star-shaped polymer for analysis of tumor suppressor protein p53 in human serum, Biosens. Bioelectron. 107 (2018) 1–9.
[22] M. Aydın, A sensitive and selective approach for detection of IL 1α cancer biomarker using disposable ITO electrode modified with epoxy-substituted polythiophene polymer, Biosens. Bioelectron. 144 (2019) 111675.
[23] B.D. Malhotra, A. Chaubey, S. Singh, Prospects of conducting polymers in biosensors, Anal. Chim. Acta 578 (1) (2006) 59–74.
[24] T. Wasilewski, W. Kamysz, J. Gębicki, Bioelectronic tongue: current status and perspectives, Biosens. Bioelectron. (2019) 111923.
[25] M. Rahman, P. Kumar, D.-S. Park, Y.-B. Shim, Electrochemical sensors based on organic conjugated polymers, Sensors 8 (1) (2008) 118–141.
[26] R. Gracia, D. Mecerreyes, Polymers with redox properties: materials for batteries, biosensors and more, Polym. Chem. 4 (7) (2013) 2206–2214.
[27] W. Lei, W. Si, Y. Xu, Z. Gu, Q. Hao, Conducting polymer composites with graphene for use in chemical sensors and biosensors, Microchimica acta 181 (7–8) (2014) 707–722.
[28] F. Teles, L. Fonseca, Applications of polymers for biomolecule immobilization in electrochemical biosensors, Mater. Sci. Eng. C 28 (8) (2008) 1530–1543.
[29] A. Ramanaviciene, A. Ramanavicius, Application of polypyrrole for the creation of immunosensors, Crit. Rev. Anal. Chem. 32 (3) (2002) 245–252.
[30] M. Gao, L. Dai, G. Wallace, Glucose Sensors Based on Glucose-Oxidase-Containing Polypyrrole/aligned Carbon Nanotube Coaxial Nanowire Electrodes, 2003.
[31] E. Tamiya, I. Karube, S. Hattori, M. Suzuki, K. Yokoyama, Micro glucose using electron mediators immobilized on a polypyrrole-modified electrode, Sensor. Actuator. 18 (3–4) (1989) 297–307.
[32] M. Yasuzawa, T. Nieda, T. Hirano, A. Kunugi, Properties of glucose sensors based on the immobilization of glucose oxidase in N-substituted polypyrrole film, Sensor. Actuator. B Chem. 66 (1–3) (2000) 77–79.
[33] A.T. Lawal, S.B. Adeloju, Polypyrrole based amperometric and potentiometric phosphate biosensors: a comparative study B, Biosens. Bioelectron. 40 (1) (2013) 377–384.
[34] I.M. Apetrei, C. Apetrei, Amperometric biosensor based on polypyrrole and tyrosinase for the detection of tyramine in food samples, Sensor. Actuator. B Chem. 178 (2013) 40–46.
[35] Z.O. Erdogan, I. Akin, S. Kucukkolbasi, A new non-enzymatic sensor based on TiO2-Ag/polypyrrole for electrochemical detection of tyramine, Synth. Met. 246 (2018) 96–100.
[36] H. Karimi-Maleh, F. Tahernejad-Javazmi, N. Atar, M.L.t. Yola, V.K. Gupta, A. A. Ensafi, A novel DNA biosensor based on a pencil graphite electrode modified with polypyrrole/functionalized multiwalled carbon nanotubes for determination of 6-mercaptopurine anticancer drug, Ind. Eng. Chem. Res. 54 (14) (2015) 3634–3639.
[37] I. Cesarino, H.V. Galesco, F.C. Moraes, M.R. Lanza, S.A. Machado, Biosensor based on electrocodeposition of carbon nanotubes/polypyrrole/laccase for neurotransmitter detection, Electroanalysis 25 (2) (2013) 394–400.
[38] R. Ramya, M. Sangaranarayanan, Polypyrrole microfibres synthesized with Quillaja Saponin for sensing of catechol, Sensor. Actuator. B Chem. 173 (2012) 40–51.
[39] S. Maeda, R. Corradi, S.P. Armes, Synthesis and characterization of carboxylic acid-functionalized polypyrrole-silica microparticles, Macromolecules 28 (8) (1995) 2905–2911.
[40] B.F. Yon-Hin, M. Smolander, T. Crompton, C.R. Lowe, Covalent electropolymerization of glucose oxidase in polypyrrole. Evaluation of methods of pyrrole attachment to glucose oxidase on the performance of electropolymerized glucose sensors, Anal. Chem. 65 (15) (1993) 2067–2071.
[41] Z. Weiss, D. Mandler, G. Shustak, A.J. Domb, Pyrrole derivatives for electrochemical coating of metallic medical devices, J. Polym. Sci. Polym. Chem. 42 (7) (2004) 1658–1667.
[42] B. Kim, L. Chen, J. Gong, Y. Osada, Titration behavior and spectral transitions of water-soluble polythiophene carboxylic acids, Macromolecules 32 (12) (1999) 3964–3969.
[43] A.C. Carreon, W.L. Santos, J.B. Matson, R.C. So, Cationic polythiophenes as responsive DNA-binding polymers, Polym. Chem. 5 (2) (2014) 314–317.
[44] M. Aydın, E.B. Aydın, M.K. Sezgintürk, A Highly Selective Poly (thiophene)-graft-Poly (Methacrylamide) Polymer Modified ITO Electrode for Neuron Specific

Enolase Detection in Human Serum, Macromolecular Bioscience, 2019, p. 1900109.
[45] E.B. Aydın, M.K. Sezgintürk, A sensitive and disposable electrochemical immunosensor for detection of SOX2, a biomarker of cancer, Talanta 172 (2017) 162–170.
[46] X. Deng, R. Nie, A. Li, H. Wei, S. Zheng, W. Huang, Y. Mo, Y. Su, Q. Wang, Y. Li, Ultra-low work function transparent electrodes achieved by naturally occurring biomaterials for organic optoelectronic devices, Advanced Materials Interfaces 1 (7) (2014) 1400215.
[47] E.B. Aydın, M. Aydın, M.K. Sezgintürk, Highly sensitive electrochemical immunosensor based on polythiophene polymer with densely populated carboxyl groups as immobilization matrix for detection of interleukin 1β in human serum and saliva, Sensor. Actuator. B Chem. 270 (2018) 18–27.
[48] W. Khan, M. Kapoor, N. Kumar, Covalent attachment of proteins to functionalized polypyrrole-coated metallic surfaces for improved biocompatibility, Acta Biomater. 3 (4) (2007) 541–549.
[49] G.E. Tranter, Protein structure analysis by CD, FTIR, and Raman spectroscopies, Encycl. Spectrosc.Spectrometry 3 (2017) 740–758. N-R third ed.
[50] M. Aydın, A sensitive and selective approach for detection of IL 1α cancer biomarker using disposable ITO electrode modified with epoxy-substituted polythiophene polymer, Biosens. Bioelectron. (2019) 111675.
[51] A. Ghosh, S. Raha, S. Dey, K. Chatterjee, A.R. Chowdhury, A. Barui, Chemometric analysis of integrated FTIR and Raman spectra obtained by non-invasive exfoliative cytology for the screening of oral cancer, Analyst 144 (4) (2019) 1309–1325.
[52] M.T. Alula, Z.T. Mengesha, E. Mwenesongole, Advances in surface-enhanced Raman spectroscopy for analysis of pharmaceuticals: a review, Vib. Spectrosc. 98 (2018) 50–63.
[53] D. Kurouski, R.P. Van Duyne, I.K. Lednev, Exploring the structure and formation mechanism of amyloid fibrils by Raman spectroscopy: a review, Analyst 140 (15) (2015) 4967–4980.
[54] M. Aydın, E.B. Aydın, M.K. Sezgintürk, A Highly Selective Electrochemical Immunosensor Based on Conductive Carbon Black and Star PGMA Polymer Composite Material for IL-8 Biomarker Detection in Human Serum and Saliva, Biosensors and Bioelectronics, 2018.
[55] L.A. Austin, S. Osseiran, C.L. Evans, Raman technologies in cancer diagnostics, Analyst 141 (2) (2016) 476–503.
[56] T. Kitagawa, S. Hirota, Raman Spectroscopy of Proteins Handbook of Vibrational Spectroscopy, Wiley, New York, 2006.
[57] I. Bruzas, W. Lum, Z. Gorunmez, L. Sagle, Advances in surface-enhanced Raman spectroscopy (SERS) substrates for lipid and protein characterization: sensing and beyond, Analyst 143 (17) (2018) 3990–4008.
[58] A. Bonifacio, C. Beleites, F. Vittur, E. Marsich, S. Semeraro, S. Paoletti, V. Sergo, Chemical imaging of articular cartilage sections with Raman mapping, employing uni- and multi-variate methods for data analysis, Analyst 135 (12) (2010) 3193–3204.
[59] M. Aydın, E.B. Aydın, M.K. Sezgintürk, Electrochemical immunosensor for CDH22 biomarker based on benzaldehyde substituted poly (phosphazene) modified disposable ITO electrode: a new fabrication strategy for biosensors, Biosens. Bioelectron. 126 (2019) 230–239.
[60] Y. Chen, B. Jiang, Y. Xiang, Y. Chai, R. Yuan, Target recycling amplification for sensitive and label-free impedimetric genosensing based on hairpin DNA and graphene/Au nanocomposites, Chem. Commun. 47 (48) (2011) 12798–12800.